

Stability and electronic structure of CdSe nanorods from first principles

T. Sadowski and R. Ramprasad*

Chemical, Materials, and Biomolecular Engineering, Institute of Materials Science, University of Connecticut, Storrs, Connecticut 06269, USA

(Received 14 May 2007; revised manuscript received 31 October 2007; published 13 December 2007)

An *ab initio* computational study was performed for wurtzite CdSe nanorods over a range of diameters and cross-sectional topologies as a function of the types of terminating surface facets. Calculations show that hexagonal cross sections containing surface atoms with one dangling bond are highly stable, possessing a large electronic band gap and exhibiting minimal surface reorientation. It is also shown that the total energy of a nanorod of arbitrary size can be approximated by an algebraic expression based on *ab initio* bulk, surface, and edge energies.

DOI: [10.1103/PhysRevB.76.235310](https://doi.org/10.1103/PhysRevB.76.235310)

PACS number(s): 71.55.Gs, 71.10.-w, 71.15.Nc, 71.20.-b

I. INTRODUCTION

As materials continue to be engineered to smaller sizes and dimensionality, many new and attractive properties have resulted. In particular, semiconductor nanocrystals (NCs) have been the subject of intense theoretical and experimental research. Current synthesis techniques allow for unprecedented control of the NC size, size distribution, and shapes leading to a diversity of geometric structures such as quantum dots,¹ nanorods,² nanobarbells,³ tetrapods,³ etc. A variety of potential applications based on these NCs are envisioned, including photovoltaic devices,⁴ lasers,⁵ biological tags,⁶ and light emitting diodes.⁷

The attractiveness of semiconductor quantum dots for photovoltaic applications is due to their ability to support a large number of electron-hole pairs (or excitons). In particular, nanostructures comprising nanorods and nanowires are arousing considerable interest⁸ since such one-dimensional structures have been shown to support a high density of excitons⁹ and offer the possibility of enhanced transport of dissociated charge carriers.¹⁰

The focus of this study is to provide a comprehensive understanding of the stability and electronic structure of CdSe nanorods, using *ab initio* computational methods. The dependence of the total energy of infinitely long CdSe nanorods in the wurtzite phase, their electronic band gaps, and the tendency of surface atoms to reorient are assessed as a function of the types of terminating surface facets of the nanorods, their cross-sectional topologies, and diameters. Consistent with our prior work on CdSe quantum dots,¹¹ we find that the most stable nanorods displaying large band gaps are those containing surface atoms with only one dangling bond. It is also shown that the total energy of a nanorod can be approximated by an algebraic expression based on *ab initio* bulk, surface, and edge energies, allowing for studies of large nanorod systems not accessible by traditional *ab initio* approaches.

II. METHODS AND MODELS

All calculations for this study were performed using the local density approximation (LDA) within SIESTA,¹² a local orbital density functional theory (DFT)¹³ code. Cadmium

and selenium core electrons were described by norm-conserving pseudopotentials of the Troullier-Martins type.¹⁴ The atomic configuration for Cd and Se were $[\text{Kr}]5s^24d^{10}$ and $[\text{Ar}3d^{10}]4s^24p^4$, respectively. A double-zeta plus polarization basis set was used for all calculations with an orbital confining cutoff radius specified by an energy shift parameter of 0.002 Ry. A set of ten special k points along the nanorod axis was found to result in well converged results. The equilibrium positions of all atoms were determined by requiring the force upon each atom to be no greater than 0.04 eV/Å.

III. RESULTS

A. Equilibrium geometry

This study considered unpassivated nanorods of CdSe based on the hexagonal wurtzite crystal structure with a and c bulk lattice constants computed to be 4.31 and 6.84 Å, respectively, in good agreement with experimental findings.¹¹ All nanorods considered here were assumed to be infinitely long with periodic length c and axis parallel to the wurtzite c axis [i.e., the (0001) direction]. A 10 Å vacuum region separated the nanorods from their periodic images along the directions normal to the nanorod axis, minimizing spurious interactions.

The (0001) nanorods considered in this study had $\{10\bar{1}0\}$ sidewall facets. $\{10\bar{1}0\}$ surfaces are nonpolar, and could have Cd and Se surface atoms with either one dangling bond (henceforth referred to as *type A* surfaces or facets) or two dangling bonds (referred to as *type B* surfaces or facets). Figure 1 shows cross sections of selected nanorods considered here which fall into three classes: (i) those with all type A sidewall facets (type A structures), (ii) those with all type B sidewall facets (type B structures), and (iii) those with alternating type A and type B sidewall facets (type AB structures). The surface energies of the type A and B facets have been previously computed and due to the difference in the number of dangling bonds of the surface atoms, the surface energy of the type A facet is lower than that of the type B facet.¹⁵

The first class of nanorods, those with type A sidewall facets, falls under three subcategories depending on whether their cross sections are regular hexagonal [Figs. 1(a) and

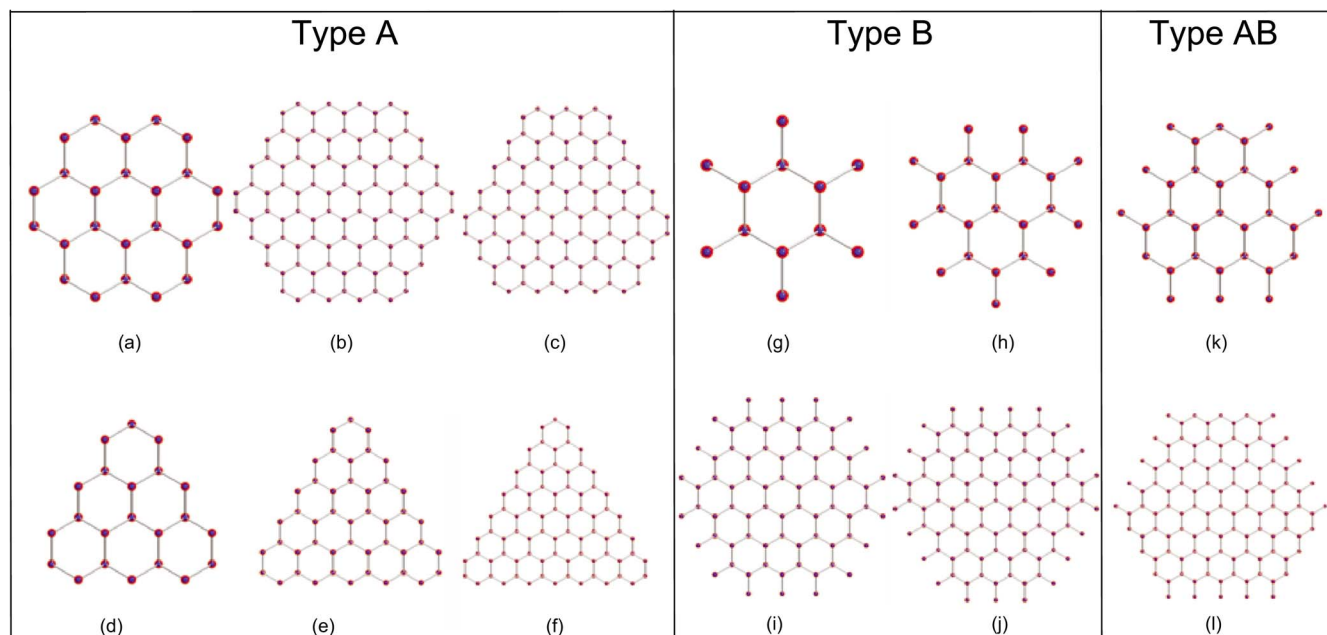


FIG. 1. (Color online) Cross-sectional topologies of selected CdSe nanorods. Cd and Se atoms are represented by red and blue, respectively.

1(b)], irregular hexagonal [Fig. 1(c)], or triangular [Figs. 1(d)–1(f)]. The smallest type A nanorod with a regular hexagonal cross section had six pairs of CdSe per supercell, and nanorods with larger diameters were successively generated by increasing the number of “shells” of hexagonal units around the central hexagon. In general, for a number of shells n , the number of CdSe pairs in a type A nanorod with a regular hexagonal cross section (H_A^R) is given by $H_A^R = 6n^2$.

A small number of type A nanorods with irregular hexagonal cross sections were also considered. These structures were generated by removing the two outermost layers of atoms on alternating facets of the type A nanorods with regular hexagonal cross sections. For instance, the nanorod of Fig. 1(c) was generated starting from that of Fig. 1(b).

The final type A subcategory of nanorods included a series of structures with triangular cross sections. The smallest such structure contained 13 CdSe pairs, with three basic hexagonal units. Figures 1(d)–1(f) show larger structures created by successively adding rows of hexagonal units. If n is the number of rows of hexagonal units, the number of CdSe pairs in a type A nanorod with a triangular cross section (H_A^T) is given by $H_A^T = n^2 + 6n + 6$ for $n > 1$. While the type A nanorods with regular hexagonal cross sections constitute nanorods with roughly spherical cross sections, those with triangular cross sections allowed for the study of a larger number of structures over the same diameter range since successive increases in the size of the latter case resulted in a smaller increase in the number of CdSe pairs.

The second class of nanorods, namely, those possessing only type B facets, was investigated in a similar manner. Removal of *just* the outermost layer of atoms from every facet of the type A nanorods resulted in the type B nanorods, with all surface atoms displaying two dangling bonds. Figures 1(g)–1(j) show selected type B nanorods. Note that the

nanorods of Figs. 1(g) and 1(i) were generated starting from those of Figs. 1(a) and 1(b), respectively.

The final class of nanorods considered was generated such that they had a hexagonal cross section, but with alternating type A and type B sidewall facets. These structures were generated by removing just the outermost layer of atoms from alternating facets of the type A nanorods with irregular hexagonal cross sections. This class of CdSe nanorods has been studied previously by Li and Wang¹⁶ and their prior work will serve as a benchmark for comparing our results.

The atomic-level geometries of all CdSe nanorods were then optimized. Figure 2 captures the changes in the atomic positions following geometry optimization for the largest type A nanorod with regular hexagonal cross section contain-

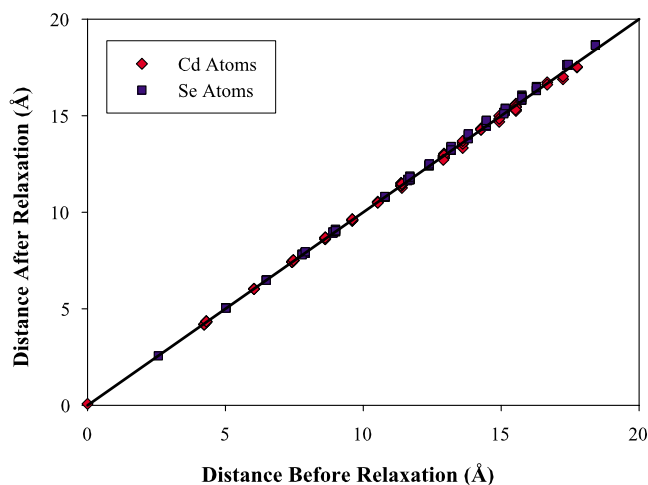


FIG. 2. (Color online) Atomic coordinate relaxation in a 96 CdSe pair type A nanorod with a regular hexagonal cross section.

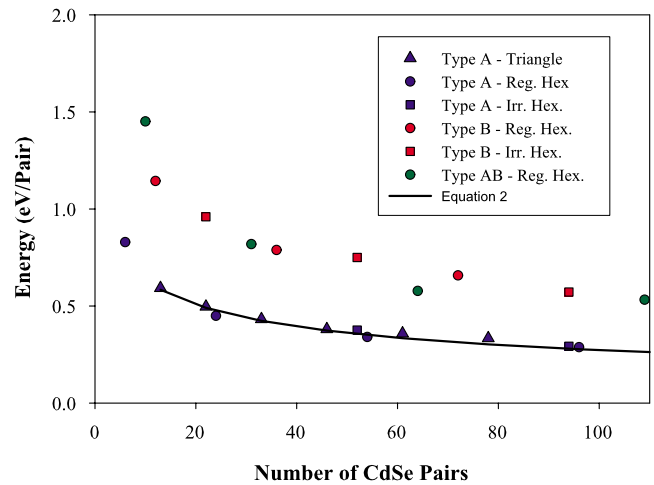
ing 96 CdSe pairs. For this system, relaxation resulted in a decrease in the total energy of -0.13 eV/pair and an increase in the band gap of 0.22 eV (to 1.46 eV) compared to the original unrelaxed geometry. It is evident that atoms in the core of the nanorod within ≈ 11 Å from the axis undergo negligible changes in position, and atoms in the outermost ≈ 8 Å thick layer undergo the maximum relaxation. Consistent with previous studies involving quantum dots¹¹ and nanorods,¹⁷ Cd atoms tend to move inward (below the straight line of Fig. 2) while the Se atoms move outward (above the line) for all nanorod topologies. In comparison with quantum dots,¹¹ the magnitude of the displacement is not nearly as great. Since our nanorods possess only two types of low energy facets, the driving force for rearrangement is much less than for quantum dots which may possess a multitude of facets that vary widely in stability.

B. Electronic structure

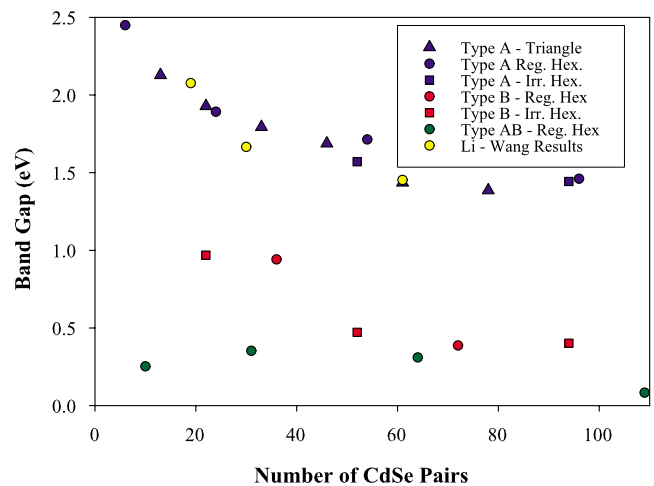
The total energies calculated for the various nanorod sizes and geometries are shown in Fig. 3(a). The trends in these diagrams confirm those in previous studies focusing on CdSe quantum dots¹¹ and quantum rods.¹⁶ For all nanorod geometries, the total energy per pair (E_{pair}) decreases with increasing nanorod size, converging to the bulk energy. In particular, the family of type A nanorods has consistently lower total energy per pair than that of any of the type B and type AB families, attributable to the single dangling bond per atom on the surface. Similarly, due to their increased number of unpassivated bonds on the surface, type B nanorods possess the highest energy per pair with type AB structures having slightly lower values. Among the type A nanorods, those with regular hexagonal cross section possessed slightly lower total energy than those with other cross sections. This can likely be attributed to gentler and more uniform variations in the angles between adjacent surface facets.

Investigation of the band gap variations with nanorod size and topologies [Fig. 3(b)] shows that, in general, the band gap increases with decreasing nanorod size, reflecting the impact of quantum confinement. These values were obtained using LDA, which tends to underestimate the band gap, especially in the II-VI family of semiconductors.¹⁶ Our calculated band gap for bulk CdSe was about 0.9 eV below the experimental value of 1.75 eV. In their study of CdSe nanorods, Li and Wang¹⁶ have used a corrected empirical pseudopotential (“LDA+C”) which accounts for the major part of the discrepancy between the LDA and experimental CdSe band gap. Based on a comparison of the LDA and LDA+C results for CdSe nanorods, they have shown that the confinement energies (the difference between the nanorod band gap and the bulk band gap) of CdSe nanorods in the 2 – 4 nm range are overestimated by LDA by about 0.18 eV. We, therefore, believe that our LDA nanorod band gaps are underestimated by a net amount of about 0.7 eV with respect to experiments. We also mention that our calculated LDA band gap values and the trends across nanorod diameters are in excellent agreement with available prior work.^{16,18}

Of the type A nanorods, those with irregular hexagonal cross sections have band gaps consistently smaller than those



(a)



(b)

FIG. 3. (Color online) (a) Total energy per pair of all CdSe nanorods studied as a function of nanorod size. The zero of energy corresponds to the CdSe bulk energy per pair. (b) Band gap as a function of nanorod size. The results of Li and Wang (Ref. 16) for passivated CdSe nanorods are also shown.

with regular hexagonal or triangular cross sections. More importantly, all type B and type AB structures possess band gap values significantly lower than comparably sized type A structures. This trend is consistent with our previous CdSe quantum dot results,¹¹ which has led to the realization that surface Cd or Se atoms displaying just one dangling bond result in no gap states and require no passivation. Surface atoms with more than one dangling bond, on the other hand, result in states in the band gap, thereby causing an apparent reduction in the band gap value.

Two pieces of supporting evidence confirm this theory. The first involves an inspection of the nanorod band structures. The left panels of Fig. 4 show the band diagrams for a type A nanorod and a type B nanorod, containing 96 and 72 CdSe pairs, respectively. While the band gap of the type A nanorod is “clean,” that of the type B nanorod contains dis-

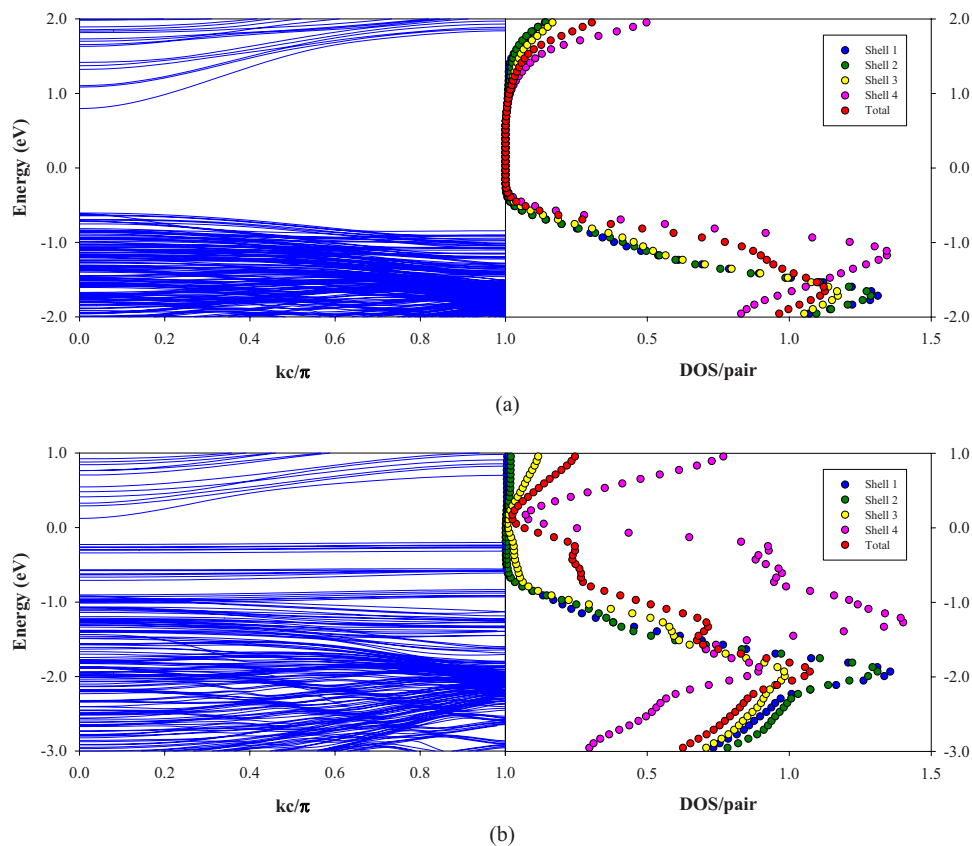


FIG. 4. (Color online) (a) Band diagram and radially decomposed density of states for a type A nanorod with regular hexagonal cross section containing 96 CdSe pairs. (b) Band diagram and radially decomposed density of states for a type B nanorod with regular hexagonal cross section containing 72 CdSe pairs.

personless bands in the band gap. The origin of these dispersionless bands or “gap states” can be traced to the surface atoms which display two dangling bonds in the type B nanorods (as opposed to just one dangling bond per surface atom in the type A nanorods). A conclusive proof of the role played by the surface atoms is provided by an analysis of the radially decomposed density of states (RDOS). The RDOS for each concentric shell of atoms in the nanorod (shown in the right panels of Fig. 4) was obtained by summing the density of states (DOS) projected from each atom in that shell [see Figs. 1(b) and 1(i)] and dividing by the total number of CdSe pairs in that shell. The innermost six CdSe pairs comprise shell 1, while the outermost layer constitutes shell 4. For the type A nanorod, the RDOS for each shell as well as the total DOS are nearly identical to one another. The surface atoms, each containing one dangling bond, behave as though the surface is completely passivated yielding a large band gap free of dispersionless bands. For the type B nanorod, the impact of an additional dangling bond per surface atom is evident when comparing the RDOS for the fourth shell to those from the inner shells. The additional peaks in the fourth shell RDOS can be correlated with the dispersionless bands in the band diagram which in general cause an apparent narrowing of the band gap of type B nanorods relative to the type A variety [Fig. 3(b)]. Thus, just as in CdSe quantum dots,¹¹ rehybridization (from sp^3 to sp^2) at surface atoms with one dangling bond keeps the band gap free of surface states in type A CdSe nanorods, while adequate rehybridization is not achieved in type B nanorods with two dangling bonds per surface atom.

The second piece of supporting evidence for our theory that single surface dangling bonds result in no surface, or gap, states is provided by prior work on CdSe nanorods.¹⁶ Li and Wang have used the charge-patching method within DFT to study a wide variety of quantum dots and rods. Their CdSe nanorods are equivalent to our type AB nanorods, but in their case, they passivate their surface atoms with pseudohydrogen atoms to saturate the dangling bonds. Their results for the band gap of three nanorods are also contained in Fig. 3(b). As can be seen, the Li and Wang results fall right on our type A nanorod results, indicating that our unpassivated type A nanorods are equivalent to type AB nanorods passivated with surface atoms to remove dangling bonds. This information provides important insight into the correlation between nanocrystal surface structure and its band gap.

IV. DISCUSSION

When considering nanorods containing a large number of atoms, traditional *ab initio* approaches may prove unfeasible due to the associated high computational costs. To evaluate the total energy of such systems, we adopt an alternate approach suggested earlier^{19–21} requiring only knowledge of the bulk, surface, and edge energies of a nanorod. As a demonstration of this approach, we consider triangular nanorods, examples of which are shown in Figs. 1(d)–1(f). The total energy of the system can be obtained through the following expression:

$$E_{tot} = \mu_{bulk} H_A^T + (3acn)\sigma + (3c)\epsilon. \quad (1)$$

H_A^T refers to the total number of CdSe pairs in the structure given as $H_A^T = n^2 + 6n + 6$, where n is the number of hexagonal unit rows in the triangular nanorod. The values a and c are the lattice constants for the wurtzite crystal and μ_{bulk} , σ , and ϵ are the bulk, surface, and edge energies, respectively. Note that for other topologies, H_A^T needs to be replaced by the appropriate expression (e.g., by H_A^R , in the case of nanorods with regular hexagonal cross section). In those cases, σ and ϵ will refer to the surface and edge energies appropriate for that topology and may be different from those determined for the triangular cross-section case. Substituting the value of H_A^T in Eq. (1), a quadratic function in n is obtained:

$$E_{tot} = (\mu_{bulk})n^2 + (6\mu_{bulk} + 3ac\sigma)n + (6\mu_{bulk} + 3c\epsilon). \quad (2)$$

Figure 3(a) contains the total energy per pair (E_{tot}/H_A^T) for the triangular nanorods with $n=2-6$. Fitting Eq. (2) to the $n=2-4$ E_{tot} DFT values resulted in $\mu_{bulk} = -1724.89$ eV/pair, $\sigma = 0.03618$ eV/Å², and $\epsilon = 0.2139$ eV/Å. The μ_{bulk} value obtained from the fit compares well with that computed by DFT for bulk CdSe (-1724.9 eV/pair). Similarly, the σ value from the fit is in good agreement with prior (10 $\bar{1}0$) surface energy computations.²² A plot of Eq. (2) is shown in Fig. 3(a)

to show the total energy of larger nanorods. In particular, E_{tot} was computed for $n=5$ and $n=6$. Compared with the DFT values, these results differed by 0.0010% and 0.0014%, respectively. Thus, this algebraic method offers a computationally efficient alternative to the more intensive, direct DFT determination of the total energies of large nanocrystals.

V. CONCLUSION

In conclusion, *ab initio* first principles calculations have been performed to examine the electronic and geometric properties of CdSe nanorods over a range of sizes and topologies. The dependence of their total energy, electronic band gaps, and the tendency of surface atoms to reorient were shown to be strongly dependent on the types of terminating surface facets. Owing to rehybridization from sp^3 to sp^2 , nanorods with surface atoms possessing one dangling bond exhibited the lowest total energy, least amount of surface reorientation, and large band gaps with their band structure devoid of gap states as though their surfaces were passivated. Finally, an alternate, accurate, and computationally efficient approach was employed to determine the total energy of a nanorod of arbitrary size requiring one-time DFT computations of bulk, surface, and edge energies.

*thomas.sadowski@uconn.edu

- ¹R. Li, J. Lee, B. Yang, D. N. Horspool, M. Aindow, and F. Papadimitrakopoulos, *J. Am. Chem. Soc.* **127**, 2524 (2005).
- ²L. Zhao, T. Lu, M. Yosef, M. Steinhart, M. Zacharias, U. Gosele, and S. Schlecht, *Chem. Mater.* **18**, 6094 (2006).
- ³A. G. Kanaras, C. Sonnichsen, H. T. Liu, and A. P. Alivisatos, *Nano Lett.* **5**, 2164 (2005).
- ⁴W. U. Huynh, J. Dittmer, and A. P. Alivisatos, *Science* **295**, 2425 (2002).
- ⁵V. I. Klimov, A. A. Mikhailovsky, S. Xu, A. Malko, J. A. Hollingsworth, C. A. Leatherdale, H. J. Eisler, and M. G. Bawendi, *Science* **290**, 314 (2000).
- ⁶W. C. Chan and S. M. Nie, *Science* **281**, 2031 (1998).
- ⁷A. P. Alivisatos, *J. Phys. Chem.* **100**, 13226 (1996).
- ⁸I. Robel, B. A. Bunker, P. V. Kamat, and M. Kuno, *Nano Lett.* **6**, 1344 (2006).
- ⁹R. D. Schaller, M. Sykora, J. M. Pietryga, and V. I. Klimov, *Nano Lett.* **6**, 424 (2006).
- ¹⁰A. J. Nozik, *Physica E (Amsterdam)* **14**, 115 (2002).
- ¹¹M. Yu, G. W. Fernando, R. Li, F. Papadimitrakopoulos, N. Shi, and R. Ramprasad, *Appl. Phys. Lett.* **88**, 231910 (2006).
- ¹²J. M. Soler, E. Artacho, J. D. Gale, A. Garcia, J. Junquera, P. Ordejon, and D. Sanchez-Portal, *J. Phys.: Condens. Matter* **14**, 2745 (2002).
- ¹³R. Martin, *Electronic Structure: Basic Theory and Practical Methods* (Cambridge University Press, New York, 2004).
- ¹⁴N. Troullier and J. L. Martins, *Phys. Rev. B* **43**, 1993 (1991).
- ¹⁵J. Y. Rempel, B. L. Trout, M. G. Bawendi, and K. F. Jensen, *J. Phys. Chem. B* **110**, 18007 (2005).
- ¹⁶J. Li and L. W. Wang, *Phys. Rev. B* **72**, 125325 (2005).
- ¹⁷D. M. Aruguete, M. A. Marcus, L. Li, A. Williamson, S. Fakra, F. Gygi, G. A. Galli, and A. P. Alivisatos, *J. Phys. Chem. C* **111**, 75 (2007).
- ¹⁸M. Li and J. C. Li, *Mater. Lett.* **60**, 2526 (2006).
- ¹⁹S. B. Zhang and S. H. Wei, *Phys. Rev. Lett.* **92**, 086102 (2004).
- ²⁰L. Manna, L. W. Wang, R. Cingolani, and A. P. Alivisatos, *J. Phys. Chem. B* **109**, 06183 (2005).
- ²¹T. M. Schmidt, R. H. Miwa, P. Venezuela, and A. Fazzio, *Phys. Rev. B* **72**, 193404 (2005).
- ²²J. Y. Rempel, B. L. Trout, M. G. Bawendi, and K. F. Jensen, *J. Phys. Chem. B* **109**, 19320 (2005).